1521-0103/12/3402-304–316
THE JOURNAL OF PHARMACOLOGY AND EXPERIMENTAL THERAPEUTICS
U.S. Government work not protected by U.S. copyright
JPET 340:304–316, 2012

Vol. 340, No. 2
185116/3741932

Characterization of Two Mutations, M287L and Q266I, in the α1 Glycine Receptor Subunit That Modify Sensitivity to Alcohols[S]

Cecilia M. Borghese, Yuri A. Blednov, Yu Quan, Sangeetha V. Iyer,[1] Wei Xiong, S. John Mihic, Li Zhang, David M. Lovinger, James R. Trudell, Gregg E. Homanics, and R. Adron Harris

Waggoner Center for Alcohol and Addiction Research, The University of Texas at Austin, Austin, Texas (C.M.B., Y.A.B., Y.Q., S.J.M., R.A.H.); Graduate Program in Molecular Pharmacology (S.V.I.) and Departments of Anesthesiology and Pharmacology and Chemical Biology (G.E.H.), University of Pittsburgh, Pittsburgh, Pennsylvania; Laboratory for Integrative Neuroscience, National Institute on Alcohol Abuse and Alcoholism/National Institutes of Health, Rockville, Maryland (W.X., L.Z., D.M.L.); and Department of Anesthesia and Beckman Program for Molecular and Genetic Medicine, Stanford University, Stanford, California (J.R.T.)

Received August 10, 2011; accepted October 27, 2011

ABSTRACT

Glycine receptors (GlyRs) are inhibitory ligand-gated ion channels. Ethanol potentiates glycine activation of the GlyR, and putative binding sites for alcohol are located in the transmembrane (TM) domains between and within subunits. To alter alcohol sensitivity of GlyR, we introduced two mutations in the GlyR α1 subunit, M287L (TM3) and Q266I (TM2). After expression in *Xenopus laevis* oocytes, both mutants showed a reduction in glycine sensitivity and glycine-induced maximal currents. Activation by taurine, another endogenous agonist, was almost abolished in the M287L GlyR. The ethanol potentiation of glycine currents was reduced in the M287L GlyR and eliminated in Q266I. Physiological levels of zinc (100 nM) potentiate glycine responses in wild-type GlyR and also enhance the ethanol potentiation of glycine responses. Although zinc potentiation of glycine responses was unchanged in both mutants, zinc enhancement of ethanol potentiation of glycine responses was absent in M287L GlyRs. The Q266I mutation decreased conductance but increased mean open time (effects not seen in M287L). Two lines of knockin mice bearing these mutations were developed. Survival of homozygous knockin mice was impaired, probably as a consequence of impaired glycinergic transmission. Glycine showed a decreased capacity for displacing strychnine binding in heterozygous knockin mice. Electrophysiology in isolated neurons of brain stem showed decreased glycine-mediated currents and decreased ethanol potentiation in homozygous knockin mice. Molecular models of the wild-type and mutant GlyRs show a smaller water-filled cavity within the TM domains of the Q266I α1 subunit. The behavioral characterization of these knockin mice is presented in a companion article (*J Pharmacol Exp Ther* **340:**317–329, 2012).

Introduction

The glycine receptor (GlyR) is an anion-conducting member of the Cys-loop family of ligand-gated ion channels. It is formed by five subunits arranged in pseudo-symmetry around a central ion-conducting pore. There are two classes of GlyR subunits, α (α1-α3 in humans) and β. The heteromeric $\alpha\beta$ GlyR is located primarily in the postsynaptic region, and the homomeric α GlyR is extrasynaptic. The stoichiometry of $\alpha\beta$ GlyR is still debated, but the most recent evidence suggests two α and three β subunits in each receptor (Lynch, 2009). Each subunit is composed of an extracellular domain, four α-helical transmembrane (TM) segments, and an intracellular loop between TM3 and TM4. Glycine binding sites are located at the interfaces between extracellular domains of different subunits, whereas the central pore is lined by the five TM2 segments (Lynch, 2009).

This work was supported by the National Institutes of Health National Institute of Alcohol Abuse and Alcoholism [Grants AA06399, AA11525, AA10422]; and the National Institutes of Health National Institute of General Medical Sciences [Grant GM47818].

Portions of this work were presented previously: Borghese CM, Mihic SJ, and Harris RA (2010) Characterization of a glycine receptor with near normal glycine function but decreased sensitivity to ethanol, at the *33rd Annual Scientific Meeting of the Research Society on Alcoholism*; 2010 June 26–30; San Antonio, TX. Research Society on Alcoholism, Austin, TX. Benavidez JM, Blednov YA, Borghese CM, Homanics GE, and Harris RA (2010) Expression of a mutant, alcohol-resistant, glycine receptor decreases alcohol sensitivity of mice, at the *33rd Annual Scientific Meeting of the Research Society on Alcoholism*; 2010 June 26–30; San Antonio, TX. Research Society on Alcoholism, Austin, TX. *Alcohol Clin Exp Res* 34:128A.

[1]Current affiliation: Waggoner Center for Alcohol and Addiction Research, The University of Texas at Austin, Austin, Texas.

Article, publication date, and citation information can be found at http://jpet.aspetjournals.org.

http://dx.doi.org/10.1124/jpet.111.185116.

[S] The online version of this article (available at http://jpet.aspetjournals.org) contains supplemental material.

ABBREVIATIONS: GlyR, glycine receptor; TM, transmembrane; WT, wild type; HEK, human embryonic kidney; ES, embryonic stem; ANOVA, analysis of variance; PCR, polymerase chain reaction; GLIC, proton-gated ion channel; CRC, concentration-response curve; bp, base pairs; kb, kilobases; aCSF, artificial cerebrospinal fluid; MBS, Modified Barth's solution.

Ethanol and other alcohols potentiate GlyR responses elicited by submaximal glycine concentrations (Celentano et al., 1988; Mascia et al., 1996). Because homomeric α GlyRs express well in heterologous systems, they have been used as prototypes of the Cys-loop family to characterize different aspects of these receptors. Using the opposing effects of ethanol in two homomeric receptors, the α GlyR and the ρ GABA receptor, a series of chimeric subunits was constructed, leading to the identification of two amino acids critical to ethanol action, one in TM2 (Ser267) and one in TM3 (Ala288) (Mihic et al., 1997). Because alcohol binding cannot be studied by traditional radiolabel binding, mutating critical amino acids to cysteine and irreversibly labeling them with thiol-specific alcohol analogs allowed the determination of specific amino acids involved in alcohol binding and action (Mascia et al., 2000). Subsequent research expanded these findings and identified critical amino acids in TM1 and TM4 (Lobo et al., 2008; McCracken et al., 2010a).

The composition of GlyR in the central nervous system undergoes a developmental change: the predominant subunit in the fetal stage is α2, which is replaced by α1 and β during the first three weeks of the postnatal stage, and these become the predominant subunits in the adult organism (Lynch, 2009). In the adult animal, α1 GlyR mRNA is predominantly located in the brain stem and spinal cord. In higher brain regions, the levels of α GlyR transcripts are considerably lower, with α1, α2, and α3 showing a differential distribution among several brain regions. The β subunit transcripts are widely and abundantly expressed throughout the central nervous system (Lynch, 2009).

Defects in glycinergic transmission can produce hyperekplexia, which is characterized by excessive startle responses and increased muscle tone, sometimes leading to death (Harvey et al., 2008; Chung et al., 2010). For instance, *oscillator* mice lack functional α1 subunits, and this frameshift mutation proves lethal for homozygous mice at approximately 3 weeks of age (Buckwalter et al., 1994; Kling et al., 1997); this illustrates that functional synaptic α1-containing GlyRs are essential for survival.

We previously constructed knockin mice with a mutation at a critical position in TM2 of the α1 subunit (S267Q) that made the GlyR insensitive to alcohol. However, the mutation also affected the normal function of the receptor, and homozygous mice did not survive (Findlay et al., 2003). We looked for other mutations that might change receptor sensitivity to alcohol or volatile anesthetic modulation, ideally without affecting other characteristics of receptor function. Two candidates were α1(Q266I) and α1(M287L) (Mihic et al., 1997). Here, we characterized these two mutations in heterologous systems (*Xenopus laevis* oocytes and HEK cells) and developed two lines of knockin mice in which we studied the electrophysiology of GlyR in brain stem neurons and radioligand binding in spinal cord and brain stem. To study the location of the mutations with respect to the previous deleterious mutation at S267Q, we built homology models of both mutated GlyRs based on the recent structure of a prokaryotic proton-gated ion channel (GLIC; Protein Data Bank ID code 3EAM) (Bocquet et al., 2009). The use of GLIC as a template for homology modeling of GlyR has been supported by two recent studies: 1) it was possible to combine the ligand-binding domain of GlyR with the TM domain of GLIC and obtain a functional chimera that gates in response to glycine (Duret et al., 2011); and 2) mutations in the TM domain of GLIC that made it resemble GlyR resulted in the enhancement of sensitivity to potentiation by ethanol at concentrations in the range of intoxication (Howard et al., 2011). The behavioral tests performed in these knockin mice are presented in a companion article (Blednov et al., 2012), and the data on volatile anesthetics will constitute another article (C. M. Borghese, Y. A. Blednov, Y. Quan, S. V. Iyer, W. Xiong, S. J. Mihic, L. Zhang, D. M. Lovinger, J. R. Trudell, G. E. Homanics, and R. A. Harris, manuscript in preparation).

Materials and Methods

Site-Directed Mutagenesis

To create the mutant α1 subunits, we introduced the single-point mutations (Q266I and M287L) into the cDNA encoding the human GlyR α1 subunit (the construct was provided by Dr. P. Schofield, Neuroscience Research Australia, Sydney, Australia), using the QuikChange site-directed mutagenesis kit (Agilent Technologies, Santa Clara, CA) with commercially produced primers (Integrated DNA Technologies Inc., Coralville, IA). Mutations were confirmed by automated fluorescent DNA sequencing (DNA Sequencing Facility, The University of Texas at Austin, Austin, TX).

Electrophysiology in X. *laevis* Oocytes

Materials. Adult female *X. laevis* frogs were obtained from Nasco (Fort Atkinson, WI). Glycine, taurine, glutamate, zinc chloride, alcohols, pentobarbital, ketamine, and flurazepam were purchased from Sigma-Aldrich (St. Louis, MO). Pentylenetetrazole was purchased from Abbott Laboratories (Abbott Park, IL), and GABA was from Sigma/RBI (Natick, MA). All other reagents were of reagent grade. Glycine and zinc chloride stocks were prepared in water. A hexanol stock was prepared in dimethyl sulfoxide and then diluted in buffer; the final dimethyl sulfoxide concentration was 0.013% (v/v), which does not affect GlyR-mediated current.

Isolation and Injection of Oocytes. The isolation and injection of the *X. laevis* oocytes and the subsequent two-electrode voltage clamp recording from them has been described previously (Lobo et al., 2008).

Drug Application Protocols. All drugs were applied by bath perfusion, and solutions were prepared on the day of the experiment. The concentration-response curves (CRCs) were obtained by applying increasing concentrations of glycine for 20 to 30 s at intervals ranging from 5 to 15 min. From these CRCs, the concentration evoking half-maximal responses (EC_{50}) were calculated, along with the Hill coefficients (see *Statistical Analysis*). To study the Zn^{2+} (100 nM), ethanol (50–200 mM), propanol (73 mM), butanol (11 mM), pentanol (2.9 mM), and hexanol (0.57 mM) modulation of glycine currents, the glycine concentration equivalent to EC_{4-6} (nominally EC_5) was determined after applying the glycine concentration that produced maximal current [3 mM for wild type (WT); 10 mM for mutant]. Washouts of 5 min were used between all glycine applications, except after maximal glycine (15 min). After two applications of EC_5 glycine, each of the modulators was preapplied for 1 min and then coapplied with glycine for 30 s. EC_5 glycine was applied between coapplications of glycine and modulator to verify the stability of glycine responses over time. The concentrations of propanol through hexanol chosen were the anesthetic EC_{50} (minimal alveolar concentration) values (Alifimoff et al., 1989). All experiments include data obtained from oocytes taken from at least two different frogs. Oocytes that presented a maximal current >20 μA were not used for data collection.

Data Analysis. Pooled data are represented as mean ± S.E.M. Statistical significance was determined by using Student's *t* test or ANOVA, as indicated. Percentage change was calculated as the percentage change from the control response to EC_5 glycine in the presence of modulator.

Nonlinear regression analysis was performed with Prism (GraphPad Software Inc., San Diego, CA). CRCs were fit to eq. 1:

$$I/I_{MAX} = \frac{1}{1 + 10^{(\log EC_{50} - \log[glycine]) \times n_H}} \quad (1)$$

where I/I_{MAX} is the fraction of the maximally obtained glycine response, EC_{50} is the concentration of agonist producing a half-maximal response, [glycine] is glycine concentration, and n_H is the Hill coefficient. Agonist responses in each cell were normalized to the maximal current that could be elicited by glycine.

Competition between glycine (full agonist) and taurine (partial agonist) was fit to eq. 2:

$$\text{Response} = \text{Bottom} + \frac{(\text{Top} - \text{Bottom})}{1 + 10^{(\log \text{taurine} - \log IC_{50})}} \quad (2)$$

where Top and Bottom are the maximal and minimal current responses observed in the curve, and IC_{50} is the concentration of taurine that gives a response halfway between the top and the bottom.

Single-Channel Recording in HEK 293 Cells

HEK 293 cells were purchased from the American Type Culture Collection (Manassas, VA). The cells were cultured in a 5% CO_2/95% O_2 atmosphere at 37°C in Dulbecco's modified Eagle's medium plus L-glutamine and sodium pyruvate (Invitrogen, Carlsbad, CA), supplemented with 10% fetal bovine serum (Gemini Bio-Products, West Sacramento, CA). They were split every 2 to 3 days by using 0.25% trypsin and 1 mM EDTA in Hanks' balanced salt solution (Invitrogen) and used through passage 15. The wild-type, Q266I, or M287L α1 GlyR cDNAs were transiently transfected with the β subunit in a 1:20 (v/v) ratio by using the PolyFect transfection reagent (QIAGEN, Valencia, CA) on 15-mm Nunc Thermanox coverslips (Cole-Parmer Instrument Co., Vernon Hills, Il) in six-well plates.

Patch-clamp electrophysiology experiments were conducted 1 to 5 days after transfection. Recording and analysis of the data were performed as described previously (Welsh et al., 2009) with some minor differences. Glycine (3 or 10 μM) was perfused over the outside-out patches. The data were low pass-filtered at 10 kHz, and a dead time of 40 μs was used.

Knockin Mouse Production

Two gene-targeting constructs were made to separately create Q266I and M287L knockin mouse lines. The Q266I construct was created essentially as described previously (Findlay et al., 2003) with the exception that site-directed mutagenesis (Quikchange II kit; Agilent Technologies) was used to change the CAG codon for glutamine at position 266 in exon 7 to ATC to encode isoleucine (see Fig. 7A). The M287L construct was also assembled from strain 129SvJ mouse genomic DNA. In brief, site-directed mutagenesis was used to change the ATG codon for methionine at position 287 of exon 8 to CTA to encode leucine (see Fig. 7B). A frt-flanked PGKneo cassette (Meyers et al., 1998) was inserted into a blunted HindIII site located ~140 bp 3′ of exon 8 (see Fig. 7C).

Both targeting constructs were linearized in the vector backbone before being separately transfected into R1 mouse embryonic stem (ES) cells (Nagy et al., 1993). ES cell culture conditions and details of electroporation and drug selection were as described previously (Homanics et al., 1997). ES cell clones were screened for gene targeting by using Southern blot analysis. In brief, for the Q266I knockin, ES cell DNA was digested with HindIII, and blots were hybridized with a 3′ probe that was external to the construct. To confirm the presence of the knockin mutations, DNA was digested with SstI and hybridized with an internal intron 7 probe. For the M287L knockin, ES cell DNA was digested with HindIII, and blots were hybridized with a 5′ external probe. The presence of the knockin mutations was verified by analyzing NheI-digested DNA that was hybridized to an internal intron 7 probe. All targeted clones were additionally analyzed in detail with multiple restriction enzymes and probes.

For the Q266I and the M287L knockin projects, the ES cell clones 198A2 and 194C2, respectively, were injected into C57BL/6J blastocyst to produce germ-line competent chimeric mice. Chimeras were bred to C57BL/6J females. Chimeras and the offspring from the aforementioned matings were crossed to FLPe-expressing transgenic mice (Rodríguez et al., 2000) (C57BL/6J genetic background) to remove the marker cassette. The FLPe transgene was subsequently bred out of both pedigrees. Within each knockin mouse line, heterozygous mice that lacked the marker gene were always crossed to produce wild-type, heterozygous, and homozygous mutant littermates for the studies described here. Thus, all mice were derived from a 129S1/X1 × C57BL/6J hybrid genetic background that was subsequently backcrossed to C57BL/6J for two generations (N2). The breeding pairs for the University of Texas colony (binding experiments) were wild type and heterozygous from the N2 mice, sent from the University of Pittsburgh. The breeding pairs for the National Institute on Alcohol Abuse and Alcoholism colony (isolated neuron electrophysiology) were heterozygous, sent from the University of Texas. Littermate mice bearing wild-type α1 GlyR subunits served as controls.

All mice were genotyped by Southern blot analysis or PCR. In brief, for the mutation at position 266, DNA was digested with SstI and hybridized with an intron 7 probe to distinguish the Gln266 wild-type allele (3.0 kb) from the Ile266 knockin allele (7.2 kb). Likewise, for the mutation at position 287, DNA was digested with NheI and hybridized with an intron 7 probe to distinguish the Met287 wild-type allele (7.5 kb) from the Leu287 knockin allele (5.7 kb). The PCR genotyping for α1(M287L) GlyR knockin mice was performed by using a forward primer (sequence: gaatcttccaggcaacatttcag) and a reverse primer (sequence: agtatcccaccaagccagtcttt) with an annealing temperature of 58°C to amplify a fragment of the genomic GlyR α1 subunit. These primers flank the GlyR α1 M287L mutation. The fragments were run on a 3% agarose gel. The wild-type gene produced one band (591 bp); homozygous knockin mice were also identified by a single band (674 bp); and heterozygous mice were observed by two bands (591 and 674 bp). The PCR genotyping for α1(Q266I) GlyR knockin mice was performed by using a forward primer (sequence: gcctgctcatcgtcatcctg) and a reverse primer (sequence: ccaatctgatctgtgcaatcct) with an annealing temperature of 55°C to amplify a fragment of the genomic GlyR α1 subunit. These primers flank the GlyR α1 Q266I mutation. The fragment was subsequently digested with SacI and run on a 3% agarose gel. The wild-type gene produced one band (701 bp); homozygous knockin mice were also identified by a single band (768 bp); and heterozygous mice were observed by two bands (768 and 701 bp). The point mutation Q266I in heterozygous or homozygous mice was observed because of the elimination of a SacI cut site by the mutation.

Mice were housed in controlled pathogen-free environments with lights on at 7:00 AM and off at 7:00 PM. Animals had unlimited access to water and rodent chow. The Institutional Animal Care and Use Committees at the University of Pittsburgh, University of Texas, and the Division of Intramural Clinical and Biological Research at the National Institute on Alcohol Abuse and Alcoholism approved all experiments.

Molecular Characterization of Knockin Mice

Spinal cords were collected from 2- to 3-week-old pups for DNA sequence analysis of reverse transcriptase-PCR products from the glycine α1 gene. Details of RNA extraction, cDNA preparation, and PCR are found in Werner et al. (2011). Glycine α1 cDNA in the region of the mutations was selectively amplified by using an exon 7 primer (5′-gctcatcgtcatcctgtcctgg-3′) and an exon 9 primer (5′-gtggtgttgttgttgttggcac3′). Additional primer pairs were used to amplify and se-

quence the entire coding region of the glycine α1 cDNA (primer sequences are available from the authors).

Tissue for Radioligand Binding Experiments

Brain stems and spinal cords from wild-type and heterozygous knockin mice were dissected and placed into 2-ml polypropylene microfuge tubes, frozen in liquid nitrogen, and kept on dry ice until storage at −70°C.

[^{3}H]Strychnine Binding

The binding procedure was similar to the one described previously (Findlay et al., 2002). For tissue homogenization, we used an Omni GLH homogenizer (Omni International, Kennesaw, GA). [^{3}H]strychnine (1.0 mCi/ml) was obtained from PerkinElmer Life and Analytical Sciences (Waltham, MA). For strychnine saturation binding assays, the final concentration of [^{3}H]strychnine in the tube was 1 to 40 nM, with or without glycine (3 mM final concentration) to measure nonspecific binding. For glycine and taurine competitive strychnine binding assays, the [^{3}H]strychnine concentration was 5 nM, glycine concentrations were between 3 and 1000 μM, and taurine concentrations were between 10 and 3000 μM. Specific [^{3}H]strychnine binding was obtained by subtracting the nonspecific (in the presence of cold 3 mM glycine) binding from the total bound radioactivity. Values for K_D, B_{max}, and Hill slope in saturation experiments, and IC_{50} and Hill slope for competitive binding assays, were determined by nonlinear regression analyses using the Prism program (GraphPad Software Inc.).

[^{3}H]Flunitrazepam Binding

Saturation binding experiments with [^{3}H]flunitrazepam were not undertaken because tritiated flunitrazepam is dissolved in ethanol, and the flunitrazepam concentrations needed would have required the presence of more than 100 mM ethanol. Homologous competitive binding experiments allow the determination of B_{MAX} and K_D by using smaller quantities of labeled ligand and displacing it with the same ligand, but in a nonradioactive form. The flunitrazepam binding procedure was similar to that described previously (Boehm et al., 2004), with some small differences. To homogenize the tissue, we added 5 ml of assay buffer and used an Omni GLH homogenizer (Omni International). [^{3}H]flunitrazepam (1.0 mCi/ml) was obtained from PerkinElmer Life and Analytical Sciences. For homologous competition binding assays, the final concentration of [^{3}H]flunitrazepam in the tube was 2 nM, and nonradioactive flunitrazepam concentrations varied between 0 and 300 nM. To determine nonspecific binding, we added flurazepam (100 μM final concentration) to tubes containing tissue plus [^{3}H]flunitrazepam. Specific [^{3}H]flunitrazepam binding was obtained by subtracting the nonspecific (in the presence of cold 100 μM flurazepam) binding from the total bound radioactivity. Values for K_D and B_{MAX} were determined by nonlinear regression analyses by using the Prism program (GraphPad Software Inc.).

Isolation of Neurons and Electrophysiological Recording

Mice (postnatal days 14–21) were sacrificed by decapitation under halothane (Sigma-Aldrich) anesthesia, and their brains were rapidly transferred to ice-cold modified artificial cerebrospinal fluid (aCSF) containing 194 mM sucrose, 30 mM NaCl, 4.5 mM KCl, 1 mM $MgCl_2$, 26 mM $NaHCO_3$, 1.2 mM NaH_2PO_4, and 10 mM D-glucose. Modified aCSF was brought to pH 7.4 by aeration with 95% O_2/5% CO_2. Brain stem slices (coronal, 300 μm thick, around the obex) were cut in ice-cold modified aCSF by using a vibrating blade microtome (Leica VT1200S; Leica Microsystems, Wetzlar, Germany) and transferred immediately to normal aCSF containing 124 mM NaCl, 4.5 mM KCl, 2 mM $CaCl_2$, 1 mM $MgCl_2$, 26 mM $NaHCO_3$, 1.2 mM NaH_2PO_4, and 10 mM D-glucose maintained at pH 7.4 by bubbling with 95% O_2/5% CO_2.

Slices were trimmed to include a portion of brain stem that contained mainly hypoglossal nucleus, but also portions of the dorsal respiratory group nuclei and the nucleus of the solitary tract. Trimmed slices were then transferred to standard external solution containing 1 mg/6 ml pronase (Sigma-Aldrich). The slices were saturated with 95% O_2/5% CO_2 and incubated at 31°C for 20 min. After an additional 20-min incubation with 1 mg/6 ml thermolysin (Sigma-Aldrich), the slices were transferred to a 35-mm culture dish. Mild trituration through heat-polished pipettes of progressively smaller tip diameters dissociated single neurons. Within 20 min of trituration, isolated neurons attached to the bottom of the culture dish were ready for electrophysiological experiments.

Recordings were made from neurons with soma diameters of 20 to 40 μM. The standard external solution contained 140 mM NaCl, 5 mM KCl, 1 mM $MgCl_2$, 2 mM $CaCl_2$, 10 mM glucose, and 10 mM HEPES (pH 7.4 with NaOH; ~320 mosmol with sucrose). With 100 mM ethanol, the pH and the osmolarity of the solution were unchanged. Patch pipette solutions contained 140 mM CsCl, 4 mM $MgCl_2$, 10 mM EGTA, 1 mM $CaCl_2$, 10 mM HEPES, 2 mM Mg-ATP, and 0.5 mM Na-GTP for conventional whole-cell recording (pH 7.2 with CsOH; ~280 mOsm with sucrose). The patch electrodes had a resistance between 1.5 and 3 MΩ when filled with the above solution.

Membrane currents were recorded in the whole-cell configuration by using an Axopatch 200B amplifier (Molecular Devices, Sunnyvale, CA) at 20 to 22°C. Cells were held at −60 mV unless otherwise indicated. Data were acquired by using pClamp 9.2 software (Molecular Devices). Data were collected at a 2-kHz digitization rate and filtered at 1 kHz. Bath solutions were applied through three-barrel square glass tubing (Warner Instruments, Hamden, CT) with a tip diameter of ~200 μm. Drugs were applied through a Warner Instruments fast-step stepper motor-driven system. The solution exchange time constants were ~4 ms for an open pipette tip and 4 to 12 ms for whole-cell recording. Neurons were exposed to ethanol alone before application of ethanol plus agonist, because this procedure maximizes the magnitude of potentiation.

Model of the GlyR

We built a homology model of α1 GlyR by threading the primary sequence of GlyR onto the X-ray structure of a prokaryotic GLIC (Protein Data Bank ID code 3EAM) (Bocquet et al., 2009). The modeling was similar to that described previously (McCracken et al., 2010a). Although the possibilities for alignment of the TM3 segment of GlyR with $GABA_A$ and nicotinic acetylcholine receptors have been a subject of some controversy (Ernst et al., 2005), we chose the "no gap" alignment of GlyR with GLIC as suggested by Bocquet et al. (2009). We used the Modeler module of Discovery Studio 2.5 (Accelrys, San Diego, CA) to build 15 models with the additional constraint that the "Cys loop" cysteines should form a disulfide bond in each subunit. We chose the "best" model based on the force field potential energy measured by CHARMm (http://www.charmm.org/). We tethered all backbone atoms and used the "side-chain refinement" module of Discovery Studio 2.5 to optimize the model. After doing so, we noted that a salt bridge could form between Arg271 in TM2 and Asp284 in TM3. Before further optimization of the model with molecular dynamics, we manually adjusted all five of these potential salt bridges to closest proximity by using the Ponder and Richards rotamer library (Ponder and Richards, 1987). We than added a distance restraint between the terminal carbon atom of each side chain (Arg171:CZ with Asp284:CG of 2.5–4.5 Å; force constant 10 kcal/Å^2). The use of the longer-distance restraint between terminal carbon atoms allows the H-bonds of the salt bridges to rotate and readjust during the molecular dynamics simulations. We added a harmonic restraint on all backbone atoms of 10 kcal/mol × Å^2, reoptimized the structure to a gradient of 0.0001 kcal/mol × Å, and performed 100,000 1-fs steps of molecular dynamics at 300°K.

We then made two "mutant" models by replacing either Q266I or M287L in only one subunit of the initial model. Each of these models was relaxed with molecular dynamics as described above. For each of the final three models, we selected the single subunit that had been mutated. We used the "define and edit binding site" module of Dis-

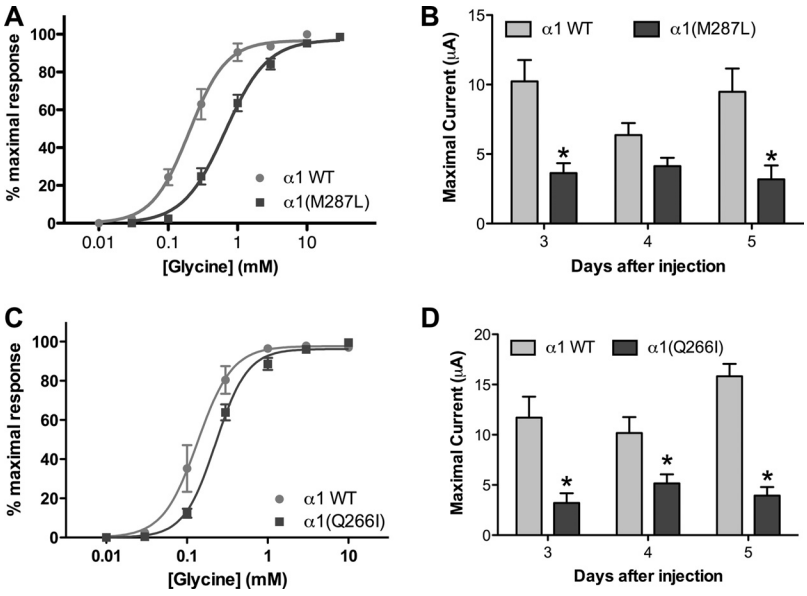

Fig. 1. Glycine responses in homomeric α1 wild type, α1(M287L), and α1(Q266I) in *X. laevis* oocytes. A and C, concentration-response curves for glycine in α1 WT and α1(M287L) (n = 5–6) (A) and α1 WT and α1(Q266I) (n = 7–8) (C) are shown. B and D, maximal glycine-induced currents in α1 WT and α1(M287L) (n = 9–49) (B) and α1 WT and α1(Q266I) (n = 6–22) (D) are shown. Two-way ANOVA and Bonferroni post hoc test were used. *, $p < 0.01$ versus corresponding WT.

covery Studio 2.5 to search for internal cavities by using a grid size of 1.0 Å and site opening of 3 Å. In each case, a single intrasubunit cavity was found. However, we found that the volume of the cavities had not changed significantly in the mutant models. Because it was possible that the harmonic restraints on the backbone atoms had prevented the models from correctly relaxing to accommodate the mutations, we subjected all three pentameric models to one million 1-fs steps of molecular dynamics at 300°K without any harmonic restraints. Then we selected just the mutated subunit from each model and used the binding site analysis module to search for internal cavities, but this time using a grid size of 0.25 × 0.25 × 0.25.

Results

Electrophysiology in *Xenopus* Oocytes

Homomeric α1 GlyRs, either WT or bearing mutations in the second [α1(Q266I)] or third TM segment [α1(M287L)], were expressed in *X. laevis* oocytes. Both mutations produced a reduction in the glycine sensitivity (Fig. 1,A and C; Supplemental Table A) and a decrease in glycine-induced maximal currents (Fig. 1, B and D).

Activation by an endogenous agonist, taurine, was recorded in buffer alone, buffer + 10 mM tricine (chelated Zn^{2+}), or buffer + 0.5 μM Zn^{2+} (physiological Zn^{2+} levels). For the latter two recording conditions, taurine responses were not changed in α1(Q266I), but were almost abolished in the α1(M287L) GlyR in all recording conditions (Fig. 2, A-C). Glycine (EC_{50}) responses recorded in the presence of increasing concentrations of taurine confirmed that taurine is a relatively efficacious partial agonist in WT GlyR but an extremely weak partial agonist in α1(M287L) GlyR, becoming essentially a competitive antagonist in the latter (Fig. 2D).

Ethanol (50–200 mM) potentiation of glycine (EC_5) currents (representative tracings in Fig. 3) was slightly reduced in the α1(M287L) GlyR (Fig. 4A) and almost completely abolished in α1(Q266I) GlyR (Fig. 4C). In contrast, longer-chain

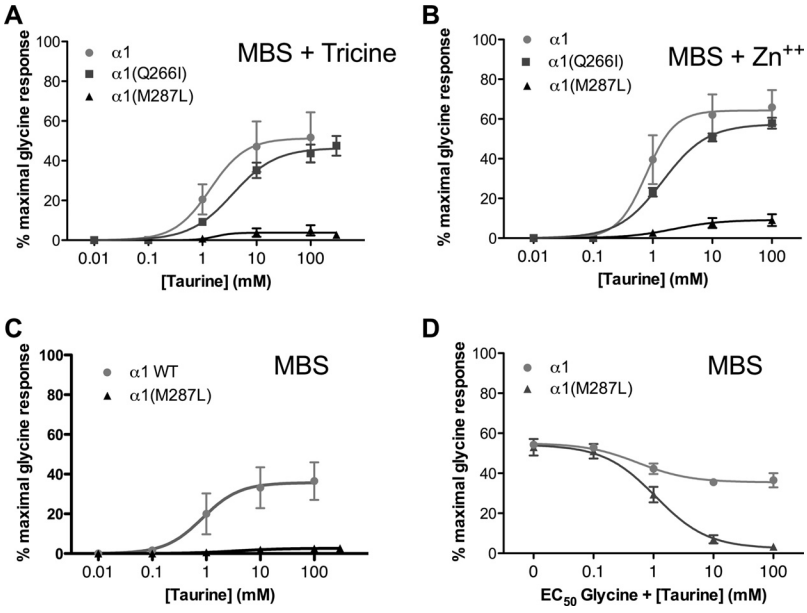

Fig. 2. Taurine responses in homomeric α1 wild type, α1(M287L), and α1(Q266I) in *X. laevis* oocytes. Concentration-response curves for taurine in Modified Barth's solution (MBS) buffer + 10 mM tricine (A), MBS buffer + 0.5 μM Zn^{2+} (B), and MBS buffer alone (C and D) are shown. Curves in D were recorded in the presence of EC_{50} glycine.

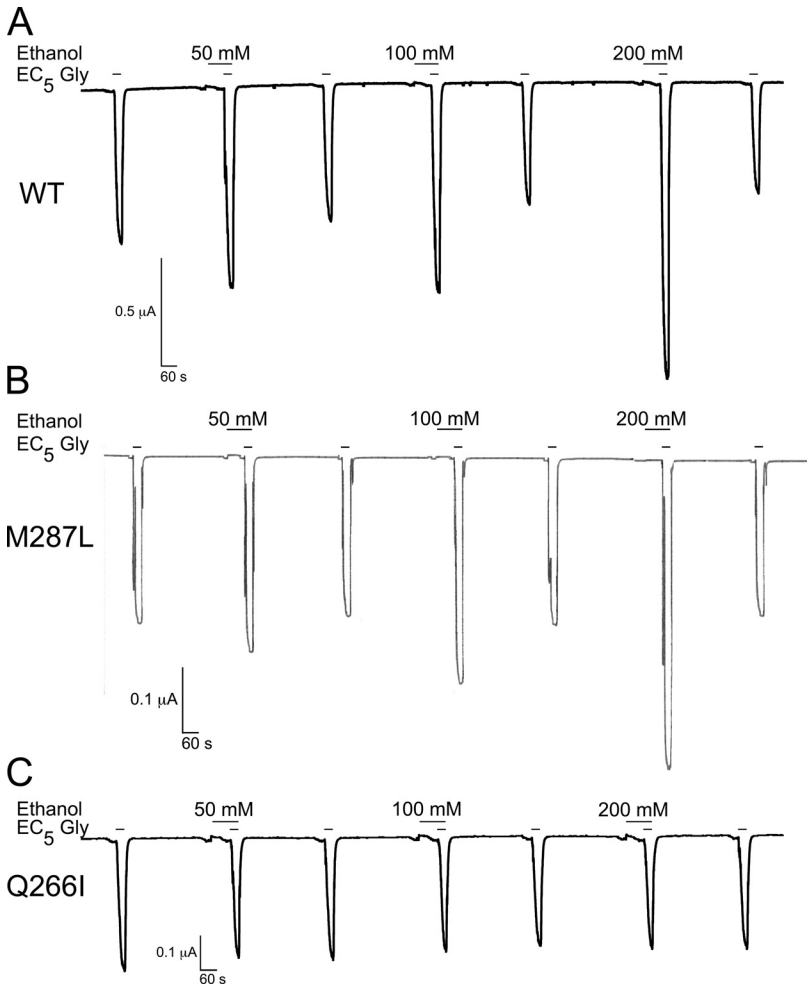

Fig. 3. Representative current traces in occytes expressing α1 GlyRs. A, wild type. B, M287L. C, Q266I. Glycine-induced currents (EC_5) in the absence and presence of ethanol (50, 100, and 200 mM) are shown.

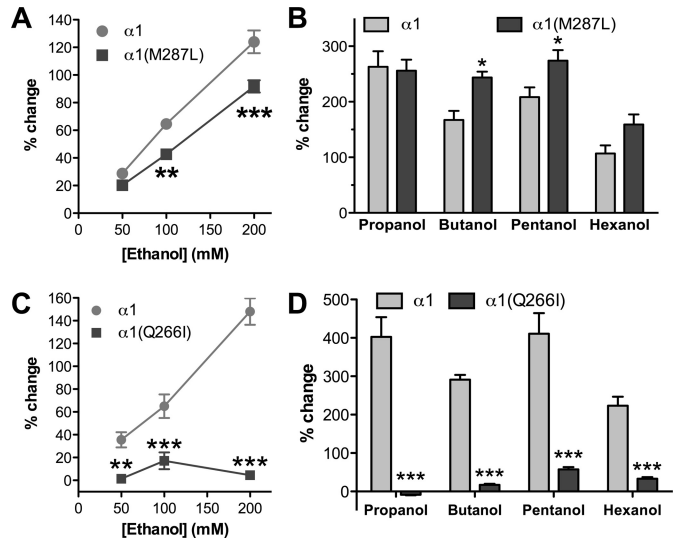

Fig. 4. Alcohol effects on homomeric α1 wild type, α1(M287L), and α1(Q266I) in *X. laevis* oocytes. A and C, concentration-response curves for ethanol potentiation of EC_5 glycine responses in α1 WT and α1(M287L) (n = 8) (A) and α1 WT and α1(Q266I) (n = 5–6) (C) are shown. B and D, alcohol potentiation of EC_5 glycine responses in α1 WT and α1(M287L) (n = 6) (B) and α1 WT and α1(Q266I) (n = 4) (D) are shown. Alcohol concentrations were: 73 mM propanol, 11 mM butanol, 2.9 mM pentanol, and 0.57 mM hexanol. Two-way ANOVA and Bonferroni post hoc test were used. *, $p < 0.05$; **, $p < 0.01$; ***, $p < 0.001$ versus corresponding WT.

alcohols showed either no difference (propanol and hexanol) or an increased potentiation (butanol and pentanol) in α1(M287L) GlyR (Fig. 4B). Four alcohols, propanol through hexanol, had very small effects on glycine responses when tested in α1(Q266I) GlyR (Fig. 4D).

Physiologically relevant levels of zinc (100 nM) potentiate glycine responses in WT GlyR and also enhance the ethanol potentiation of glycine responses (McCracken et al., 2010b). Although the zinc potentiation of glycine responses was unchanged in the α1(M287L) GlyR (Fig. 5A), zinc enhancement of ethanol potentiation of glycine responses was absent (Fig. 5B). However, the zinc enhancement of butanol potentiation of glycine responses was unchanged in α1(M287L) GlyR (Fig. 5C). The zinc potentiation of glycine responses was similar in α1 WT and α1(Q266I), but the coapplication of zinc and ethanol did not change the ethanol effect on the mutant receptor: that is, even in the presence of zinc, ethanol did not change the glycine response (data not shown).

To test whether the mutations modified the sensitivity of the GlyR to other modulators, we used several drugs that are either known to modify the GlyR function or that we planned to test in the knockin mice. The mutations did not induce changes in the sensitivity to ketamine, flurazepam, pentylenetetrazole, or glutamate; all of these compounds produced only minimal effects in the mutant GlyRs as well as in the wild type (Supplemental Table B). It is noteworthy that we did not observe the recently reported potentiation of GlyR-

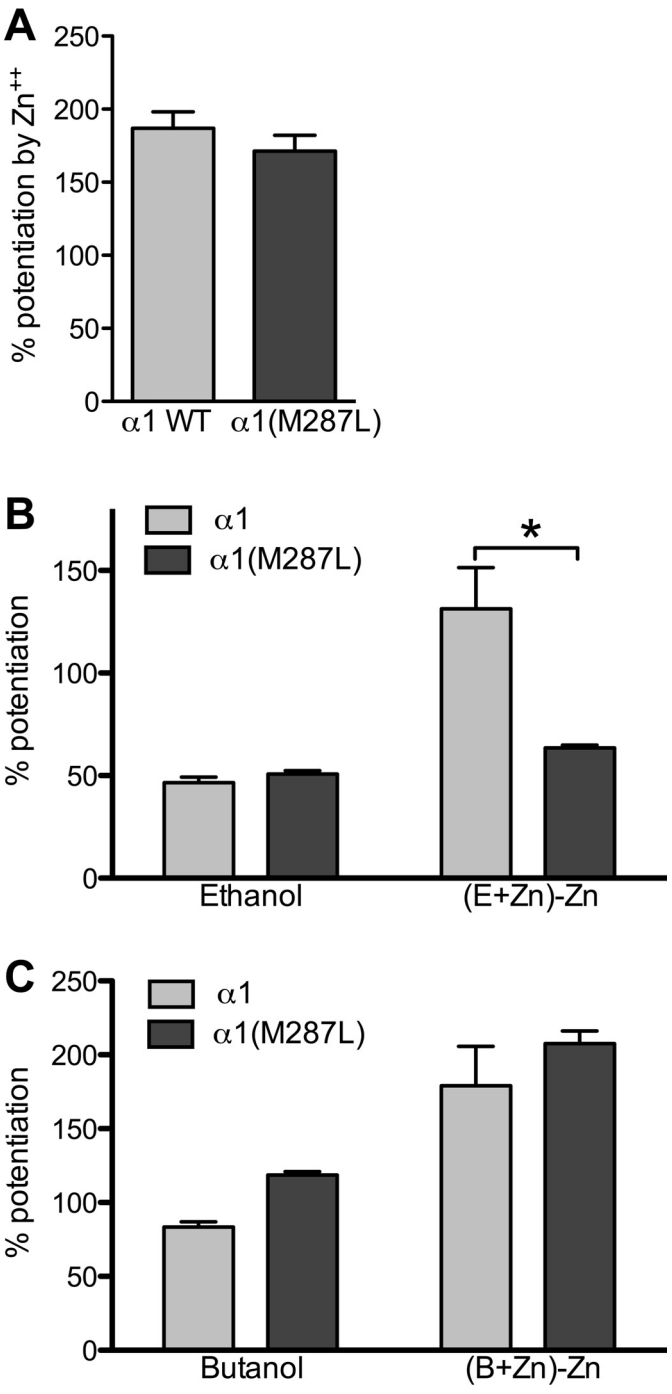

Fig. 5. Zinc effect on glycine responses and ethanol enhancement of glycine responses in homomeric α1 wild type, α1(M287L), and α1(Q266I) in *X. laevis* oocytes. A, 100 nM Zn^{2+} potentiation of EC_5 glycine responses. B, ethanol effect and Zn^{2+} enhancement of ethanol potentiation on EC_5 glycine responses, calculated as the potentiation seen when ethanol and Zn^{2+} are coapplied with glycine (E+Zn) minus the enhancement observed when only Zn^{2+} is applied with glycine. C, butanol and Zn^{2+} enhancement of butanol potentiation on EC_{4-6} glycine responses, calculated as described above. Two-way ANOVA and Bonferroni post hoc test were used. *, $p < 0.001$ versus corresponding wild type.

mediated currents by glutamate (Liu et al., 2010), but instead found a small inhibition. GABA produced a small inhibition of glycine responses, slightly increased in α1(M287L) versus the wild type. The most notable effect of the mutations was seen with pentobarbital. We found that pentobarbital potentiation of glycine responses was small in the wild type (11%), enhanced in α1(M287L) (52%), and switched to slight inhibition in α1(Q266I) (−8%).

Single-Channel Recordings

Outside-out patch single-channel recordings were obtained from HEK 293 cells transiently transfected with cDNAs encoding for α1 and β GlyR subunits (Fig. 6). WT αβ GlyR were exposed to 3 μM glycine, whereas the two mutants (slightly less sensitive to glycine) were exposed to 10 μM glycine. The sample tracings in Fig. 6A illustrate that the mutations quite markedly affected the properties of these channels. Although the M287L mutation slightly decreased the mean open channel lifetime (Fig. 6B), the major effect of the mutation seemed to be a prolongation of bursts of channel-opening activity (Fig. 6A). Like WT receptors, the M287L heteromeric GlyR displayed a main conductance of 47 pS, although a subconductance state was also occasionally noted as shown in the last line of the M287L tracing (Fig. 6A). The Q266I mutation, in contrast, markedly increased the mean channel open time (Fig. 6B) compared with WT and M287L receptors ($F_{2,8} = 25.4$; $p < 0.001$) and decreased the conductance to 33 pS. For all receptors, the open and closed dwell-time data could be described by using three and four exponential components, respectively. The two longest open dwell times (τ2 and τ3) were increased in the Q266I α1β GlyR (Fig. 6C), and the likelihood of opening to the longest-lived open time component seemed higher in the Q266I receptor (Fig. 6D), explaining the higher mean open time in this mutant.

Knockin Mice

Two separate gene-targeting experiments were conducted to create two independent GlyR α1 subunit knockin mouse lines (Q266I or M287L knockin). Wild-type ($\alpha1^{Q/Q}$ or $\alpha1^{M/M}$), heterozygous ($\alpha1^{Q/I}$ or $\alpha1^{M/L}$), and homozygous ($\alpha1^{I/I}$ or $\alpha1^{L/L}$) littermates were compared.

As shown in Fig. 7, D and E, DNA sequence analysis of reverse transcription-PCR products derived from mRNA isolated from the spinal cord of the mice established that the intended mutations were introduced into the α1 subunit of the glycine receptor and were expressed. The entire coding region of the α1 subunit was analyzed, and no other sequence differences existed between the controls and the mutants (data not shown).

Genotype analysis of offspring derived from heterozygous matings revealed that knockin mice were born at the expected 1:2:1 frequency. For the Q266I knockin, the genotype distribution of offspring was $\alpha1^{Q/Q}$ ($n = 8$), $\alpha1^{Q/I}$ ($n = 15$), and $\alpha1^{I/I}$ ($n = 10$). For the M287L knockin, the genotype distribution was $\alpha1^{M/M}$ ($n = 13$), $\alpha1^{M/L}$ ($n = 30$), and $\alpha1^{L/L}$ ($n = 15$). Thus, the knockin mutations did not affect in utero survival.

However, postnatal survival was severely affected by the knockin mutations, especially for the Q266I knockin. $\alpha1^{I/I}$ mice displayed a noticeable phenotype beginning approximately postnatal day 10. By postnatal day 14, all $\alpha1^{I/I}$ mice were phenotypically abnormal and overtly distinguishable from $\alpha1^{Q/Q}$ and $\alpha1^{Q/I}$ littermates. The phenotype consisted of muscle tremor and motor control abnormalities that prevented normal postural control and severely curtailed locomotion. These motor abnormalities probably prevented normal feeding behavior and resulted in the marked reduction in body weight that was observed [2-week body weights: $\alpha1^{Q/Q}$

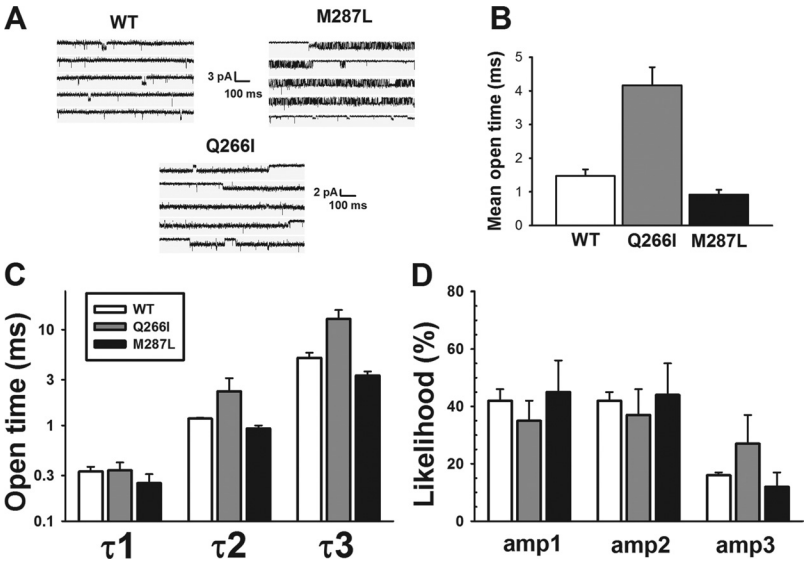

Fig. 6. Effects of α1 subunit mutation on single-channel properties. A, representative single-channel responses of wild-type, Q266I, and M287L α1β GlyRs to continuous perfusion of 3 μM (WT) or 10 μM (Q266I and M287L) glycine. B, the Q266I mutation significantly increases mean channel open lifetime. C, open dwell-time data from all three receptors could be fit to three components, with only the Q266I mutation affecting the two longer-lived components. D, the likelihoods of occurrence of each of the three open time components did not vary greatly except for a higher likelihood of the Q266I-containing GlyR to open to the longest-lived state (amp3).

and $\alpha1^{Q/I}$, 8.1 ± 0.2 g (n = 13) versus $\alpha1^{I/I}$, 4.2 ± 0.2 g (n = 3)]. All $\alpha1^{I/I}$ mice died or were sacrificed for humane reasons between 2 and 3 weeks of age. $\alpha1^{Q/I}$ mice displayed a mild phenotype and were distinguishable from $\alpha1^{Q/Q}$ controls by their display of hind leg clasping behavior when held by the tail. All $\alpha1^{Q/I}$ mice tested (n = 38) between ~2 and 10 weeks of age displayed leg clasping behavior compared with 0 of 27 $\alpha1^{Q/Q}$ mice.

The M287L knockin mutation was somewhat less deleterious. $\alpha1^{L/L}$ mice displayed intermittent muscle tremors and postural control issues that were similar, but less severe compared with the $\alpha1^{I/I}$ mice described above. Survival was markedly reduced. Of five $\alpha1^{L/L}$ mice that were closely monitored, one died at 5 weeks of age, three died at 11 to 12 weeks of age, and one survived until 14 weeks when the study was terminated. Body weights were also significantly reduced in $\alpha1^{L/L}$ mice compared with $\alpha1^{M/M}$ controls starting around 3 weeks of age (males: 9.5 ± 0.2 g versus 10.9 ± 0.3 g, respectively; $p < 0.05$). By 10 weeks of age, body weight of $\alpha1^{L/L}$ mice was ~44% less than $\alpha1^{M/M}$ (males: 16.8 ± 0.7 g versus 29.1 ± 0.6 g, respectively; $p < 0.0001$).

Radioligand Binding Experiments

[^{3}H]Strychnine Binding. Strychnine is a high-affinity, competitive antagonist of GlyRs. Binding of tritiated strychnine to glycine receptors present in membranes from brain stem and spinal cord showed no difference between WT and knockin mice: neither B_{MAX} nor K_D were different (Supplemental Table C). However, there were significant differences in competitive binding experiments: both glycine and taurine were less potent in competing with tritiated strychnine for their binding site in tissue from heterozygous $\alpha1^{M/L}$ mice than in WT $\alpha1^{M/M}$ mice (Supplemental Table C). For heterozygous $\alpha1^{Q/I}$ mice, only glycine showed less potency in competing with strychnine; there was a trend for taurine to show a decreased potency, but it did not reach statistical significance (Supplemental Table C). In membranes from both WT and knockin mice, high concentrations of glycine and taurine completely displaced strychnine from the binding sites.

[^{3}H]Flunitrazepam Binding. Flunitrazepam binds with high affinity to a well characterized binding site present in $GABA_A$ receptors containing α1/2/3/5 and γ subunits. Using tissue from WT $\alpha1^{Q/Q}$ and heterozygous $\alpha1^{Q/I}$ mice, tritiated flunitrazepam was displaced by increasing concentrations of flunitrazepam, and B_{MAX} and K_D were determined. There was no difference between the WT and knockin parameters (Supplemental Table C), suggesting that the flunitrazepam binding sites in the $GABA_A$ receptors were not affected by the GlyR mutations.

Electrophysiology in Neurons of Knockin Mice

Neurons from the brain stem of mutant and control mice were acutely isolated. Using the whole-cell recording technique, currents elicited by glycine application in the presence or absence of ethanol were recorded (representative tracings in Fig. 8). The application of increasing concentrations of glycine produced concentration-response curves that were similar for WT and heterozygous knockin mice (Fig. 9A). The magnitude of the maximal glycine-induced currents depended on the genotype: maximal currents in homozygous knockin mice were smaller than in WT for both mutants; for heterozygous knockin mice, only the Q266I mutation decreased the maximal current (Fig. 9B).

Application of ethanol alone had no effect on baseline current amplitude (before glycine application) in neurons from mice of either genotype. The ethanol potentiation of submaximal glycine currents was decreased for the knockin mice, both heterozygous and homozygous (Fig. 9, C and D). Remarkably, ethanol potentiation was essentially absent in neurons from homozygous knockin mice.

Models of the Q266I and M287L Mutations in GlyR

The mutations in GlyR have a relatively small effect on the backbone structure of the receptor. Superimposition of the structures showed that most deviations originated in the N- and C-terminal ends of the structure (Fig. 10E). However, a detailed view of the region surrounding Gln266, Ser267, Met287, and Ala288 (Fig. 10, A-C) showed small differences in the spacing between the residues. In these models, the residues previously implicated as important to alcohol and anesthetic modulation (Mihic et al., 1997), Ser267 and Ala288, are not directly pointed into the center of the intrasubunit four-helical bundle. Instead, Ser267 is pointed to-

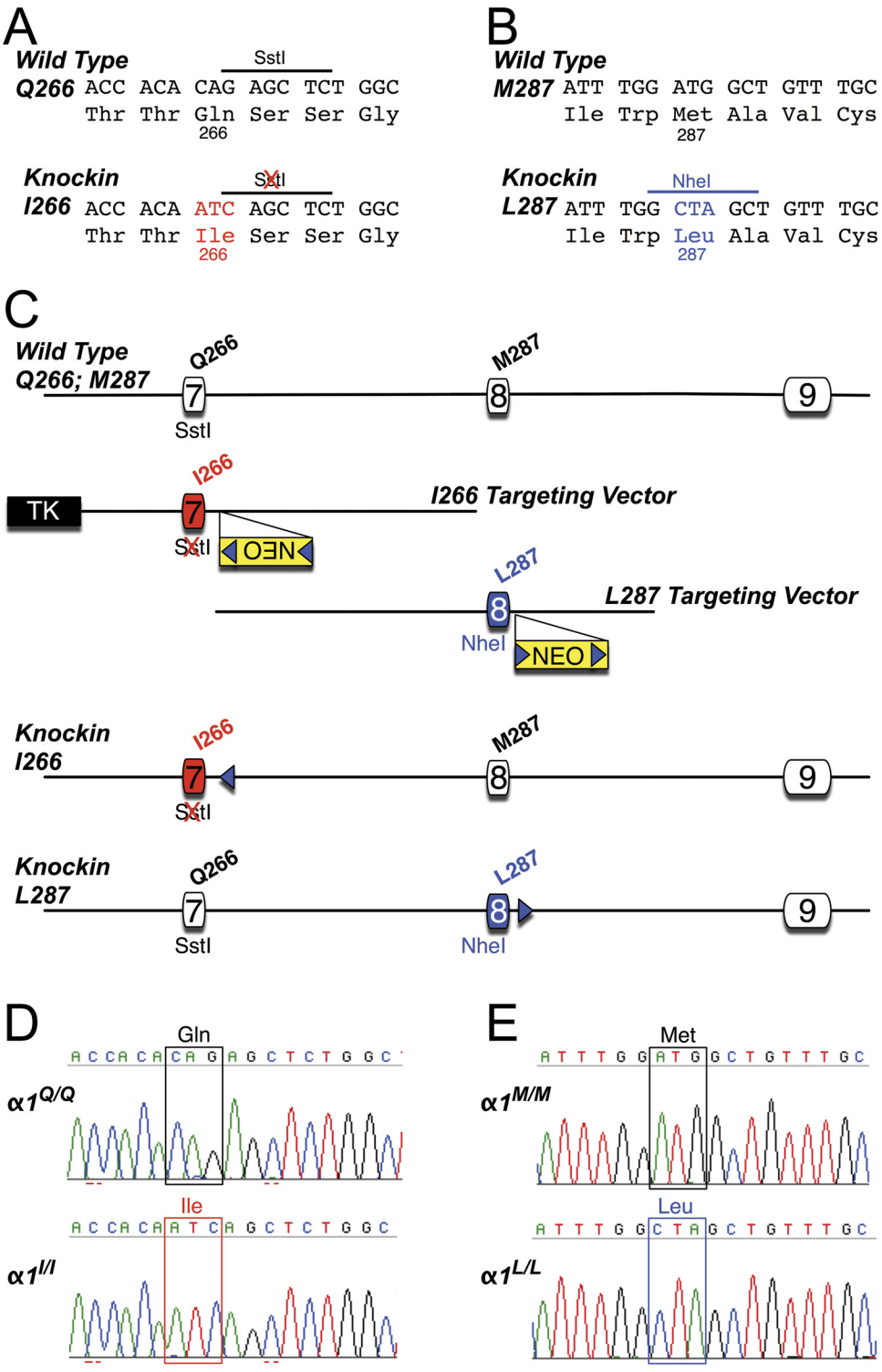

Fig. 7. Production of glycine α1 gene-targeted knockin mice. A, partial DNA sequence of exon 7 of the wild-type (Gln266) and mutant (Ile266) α1 genes. Note that amino acid 266 encoded by the wild-type sequence is glutamine (Gln) but in the knockin sequence the three nucleotides in red change this codon to isoleucine (Ile). These alterations also destroy a SstI restriction endonuclease recognition site. B, partial DNA sequence of exon 8 of the wild-type (Met287) and mutant (Leu287) α1 genes. Note that amino acid 287 encoded by the wild-type sequence is methionine (Met) but in the knockin sequence the three nucleotides in blue change this codon to leucine (Leu). These alterations also introduce a NheI restriction endonuclease recognition site. C, strategy used to modify the glycine α1 locus in embryonic stem cells. Exons 7 and 8 correspond to nucleotides 698 to 912 and 913 to 1059, respectively (nucleotide 1 corresponds to the start of translation) of the mouse cDNA (Ensembl Transcript ID: ENSMUST00000075603). Illustrated, from top to bottom, are the wild-type allele, the targeting vector used to create the Ile266 knockin, the targeting vector used to create the Leu287 knockin, the Ile266 knockin allele after FLPe-mediated deletion of the frt (blue triangles) flanked selectable marker cassette (NEO), and the Leu287 knockin allele after NEO deletion. D and E, DNA sequence analysis of glycine receptor α1subunit reverse transcription-PCR products from spinal cord of homozygous $\alpha1^{Q/Q}$ control and $\alpha1^{I/I}$ knockin mice (D) and $\alpha1^{M/M}$ control and $\alpha1^{L/L}$ knockin mice (E). These results demonstrate that the introduced mutations are present in the α1 gene products that are expressed in spinal cord of knockin mice. Multiple overlapping PCR products that spanned the coding region were analyzed, and no other differences between genotypes were present.

ward the TM3 α helix and Ala288 is pointed toward the intersubunit space. However, now Gln266 and Met287 point inward into the center of the four-helical bundle.

A cavity-finding program was used to identify putative binding cavities in a single subunit of the WT and mutated GlyRs, after running molecular dynamics in the three pentameric models without any harmonic restraint on the backbone atoms. The algorithm identified one intrasubunit cavity per model. The cavity volumes were depicted as a green van der Waals surface (Fig. 10, D-F) and measured after the unrestrained molecular dynamics by using a 0.25 × 0.25 × 0.25 cubic grid. The respective cavity volumes were 216 Å^3 for WT (Fig. 10D), 234 Å^3 for M287L (Fig. 10F), and a considerably smaller 168 Å^3 for Q266I (Fig. 10E).

Discussion

We studied two single-point mutations in the GlyR: α1(M287L) and α1(Q266I). After expressing them in heterol-

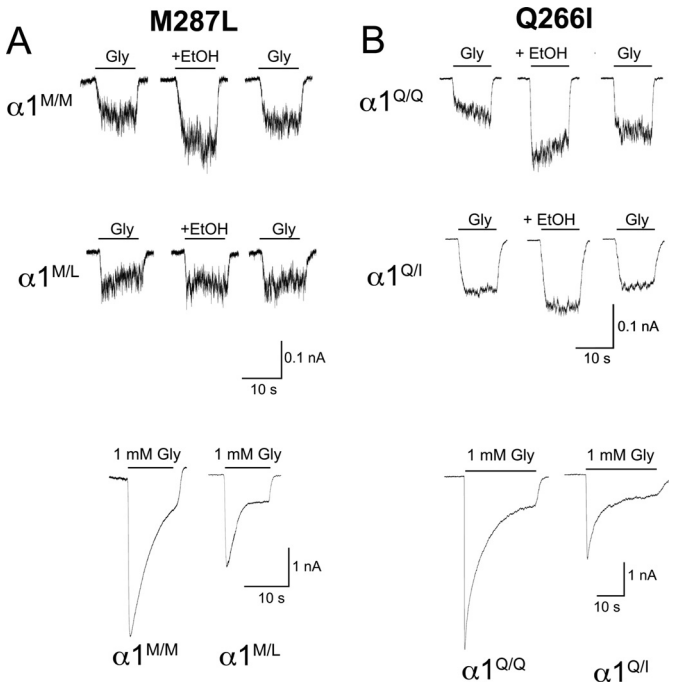

Fig. 8. Representative current traces in neurons of α1 GlyR knockin mice [M287L (A) and Q266I (B)]. The top trace records are glycine-induced currents (10 μM glycine) before, during, and after 100 mM ethanol (EtOH). The bottom trace records are maximal glycine-induced currents (1 mM glycine). $\alpha1^{M/M}$ and $\alpha1^{Q/Q}$, wild-type mice; $\alpha1^{M/L}$ and $\alpha1^{Q/I}$, heterozygous knockin mice.

ogous systems (*X. laevis* oocytes and HEK 293 cells), we found that the mutated receptors presented several differences in their sensitivities to glycine, taurine, alcohols, and anesthetics compared with the WT GlyR (summarized in Table 1).

Both mutations introduced sufficient alterations in the function of the GlyR to cause the death of mice homozygous for the mutations. Several effects of the mutations might contribute to the lethality. In both mutants, there was a reduction in the sensitivity to glycine (increased EC_{50}) in homomeric mutated GlyRs expressed in oocytes. The absence of a change in glycine sensitivity observed in neurons from heterozygous mice could be caused by the "dilution" of mutated α1 subunits with WT α1 and β subunits. However, a decrease in glycine sensitivity was also found in the α1(D80A) mice, yet the homozygous α1(D80A) mice lived beyond 2 to 3 weeks postnatally (Hirzel et al., 2006). Both mutant GlyRs also displayed a decrease in the magnitude of glycine-induced maximal currents in both oocytes and neurons, as was the case for the α1(S267Q) knockin mice, and all three mutations proved lethal in the homozygous mice (Findlay et al., 2003). The α1(Q266I)β GlyR showed a decreased conductance compared with α1β WT and α1(M287L)β receptors, probably because the 266 residue is found in the TM2 segment that lines the pore, and in that position, it is more likely to influence conductance than the 287 residue found in TM3. The maximal currents measured in neurons from heterozygous and homozygous mice reflect this difference: in neurons from homozygous knockin mice there is a significant reduction in maximally evoked currents in both lines, but in neurons from heterozygous mice, a significant reduction is seen only in neurons from $\alpha1^{Q/I}$ mice. There are several mutations in the α1 GlyR subunit that cause hyperekplexia and also show decreased conductance: R271L and R271Q (TM2–3 loop), and P250T (TM1–2 loop) (Rajendra et al., 1995; Breitinger et al., 2004). In contrast, there is no change in conductance in α1(Q266H) or α1(A52S) *spasmodic* mice (Moorhouse et al., 1999; Plested et al., 2007). In summary, both mutations probably cause early death in homozygous mice because of the decreased maximal glycinergic currents. This may be caused in part by a decrease in the GlyR trafficking, as has been observed for other α1 mutations that cause hyperekplexia (Villmann et al., 2009), as well as a decrease in conductance in the case of α1(Q266I).

As summarized in Table 1, the results from the different techniques (electrophysiology in both *X. laevis* oocytes and neurons, and the strychnine binding in homogenates from heterozygous knockin mice) are consistent with some previous studies of mutant mice. Specifically, the decreased sensitivity to glycine, the conversion of taurine from partial agonist to competitive antagonist, and the decrease in gly-

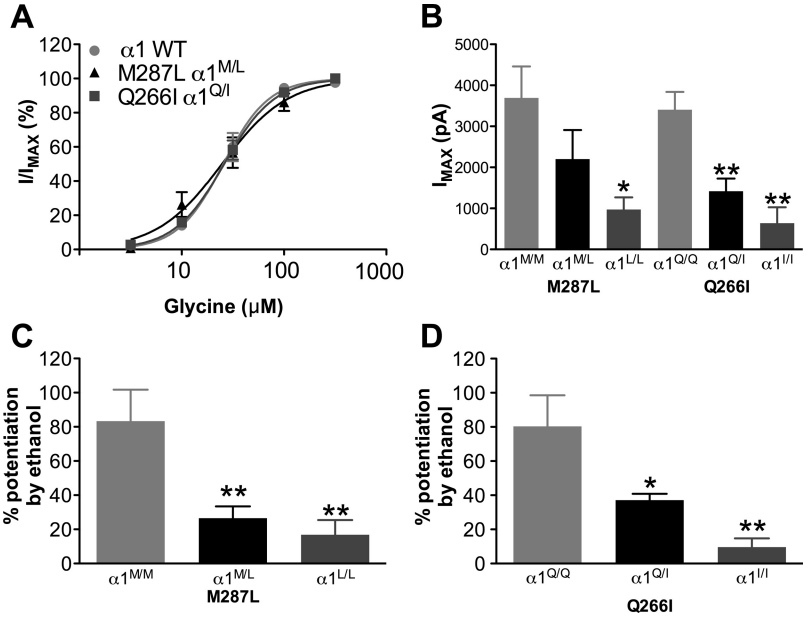

Fig. 9. Glycine-induced currents in neurons of α1 GlyR knockin mice (M287L and Q266I). A, glycine concentration-response curves in neurons from WT and heterozygous mice ($n = 4$). B, maximal glycine-induced currents ($n = 6–8$). C and D, ethanol (100 mM) potentiation of glycine currents (10 μM glycine, 5–7 mice from each animal line). *, $p < 0.05$; **, $p < 0.01$ versus corresponding WT mice. One-way ANOVA followed by Dunnett's post hoc test was used. α1 WT, $\alpha1^{M/M}$, and $\alpha1^{Q/Q}$, wild-type mice; $\alpha1^{M/L}$ and $\alpha1^{Q/I}$, heterozygous knockin mice; $\alpha1^{L/L}$ and $\alpha1^{I/I}$, homozygous knockin mice.

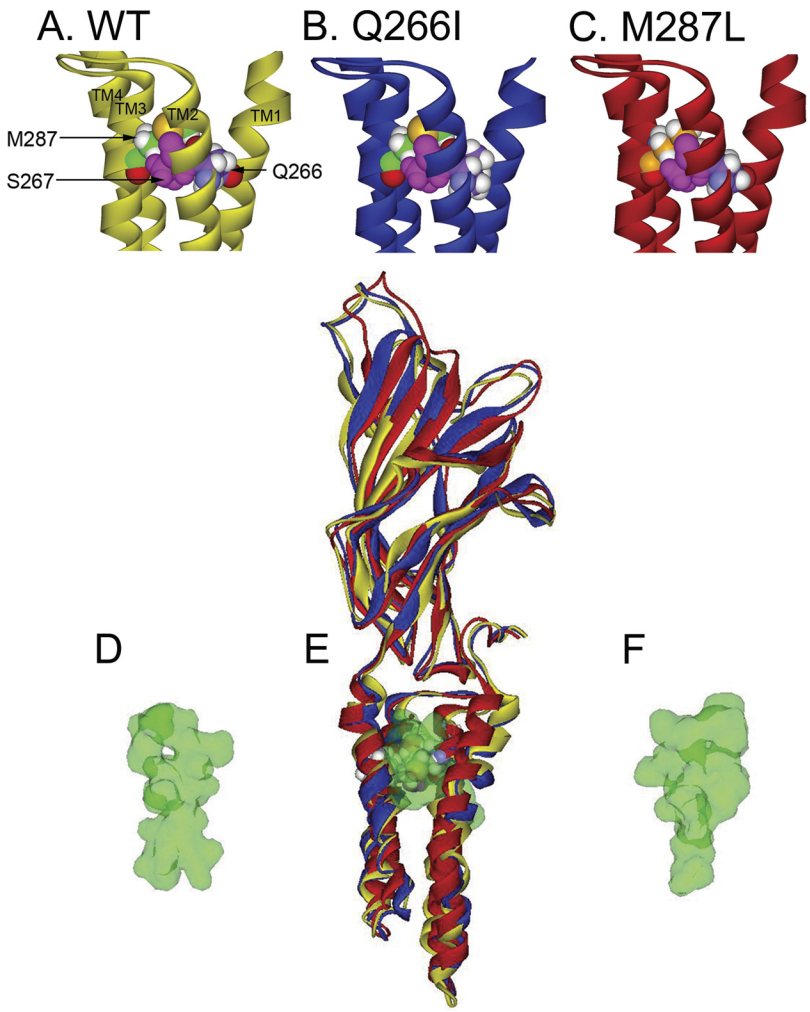

Fig. 10. Homology model of M287L and Q266I mutations in GlyR. A to C, homology models of GlyR, A, a detailed view of the region surrounding Gln266 (violet, carbon atoms; red, oxygen atoms; white, hydrogen atoms), Ser267 (used as reference point, all atoms pink), and Met287 (green carbon atoms) in the WT subunit. B and C, the Q266I (B; violet carbon atoms) and the M287L (C; orange carbon atoms) mutations revealed only small differences in the spacing between the residues. The view is from the center of the ion pore. D to F,. a cavity-finding program was used to identify putative binding cavities in a single subunit of the WT and mutated GlyRs, after subjecting the models to molecular dynamics without harmonic restraints on the backbone atoms. The algorithm identified one within-subunit cavity per model. The cavity volume in the WT (D), Q266I (E), and M287L (F) subunits is depicted as a green van der Waals surface. The view is from the plane of the membrane, with TM1 (on the left) and TM4 (on the right) of each subunit in the foreground, allowing a better view of the within-subunit cavity. In E, the ribbons representing the full WT and mutated subunits are depicted overlaid to one another.

cine- and taurine-induced displacement of strychnine binding, without changes in the strychnine binding per se, all have been observed in other mutations that cause deficits in the glycinergic transmission (Saul et al., 1994; Rajendra et al., 1995; Moorhouse et al., 1999; Castaldo et al., 2004; Becker et al., 2008).

The decreased glycine-induced maximal currents observed in both oocytes [homomeric α1(M287L) and α1(Q266I) GlyRs]

TABLE 1
Comparison of results from different tests for α1 GlyR mutations M287L and Q266I

Electrophysiology in Oocytes, Homomeric α1 GlyRs	Strychnine Binding, Spinal Cord + Brain Stem from Heterozygous Mice	Electrophysiology in Isolated Neurons, Brain Stem
M287L		
Reduced glycine potency, increased EC_{50}	Reduced displacement by glycine, increased IC_{50}	Heterozygous: similar glycine potency, same EC_{50}
Reduced maximal glycine current amplitude	No changes in strychnine B_{MAX}	Heterozygous: no change in maximal glycine current amplitude; homozygous: reduced maximal glycine current amplitude
Reduced taurine potency, increased EC_{50}	Reduced displacement by taurine, increased IC_{50}	Not tested
Reduced taurine efficiency, decreased I_{MAX}	No equivalent	Not tested
Reduced zinc-enhacement of ethanol potentiation	Not tested	Reduced ethanol potentiation, existing zinc in the buffer
Q266I		
Reduced glycine potency, increased EC_{50}	Reduced displacement by glycine, increased IC_{50}	Heterozygous: similar glycine potency, same EC_{50}
Reduced maximal glycine current amplitude	No changes in strychnine B_{MAX}	Heterozygous and homozygous: reduced maximal glycine current amplitude
Abolished ethanol potentiation	Not tested	Heterozygous: reduced ethanol potentiation; homozygous: abolished ethanol potentiation

and isolated neurons (homozygous $\alpha1^{L/L}\beta$ and $\alpha1^{I/I}\beta$ GlyRs) in both lines of knockin mice were not reflected in the strychnine binding results. B_{MAX} values in the strychnine binding and the maximal displacement of strychnine binding by glycine were similar for WT and knockin mice. A similar apparent contradiction has been observed in other α1 GlyR mutations (Langosch et al., 1994; Rajendra et al., 1995). For Q266I, it could be a result of the decreased conductance of the mutated GlyR. For M287L, strychnine binding in homogenates may label the total number of GlyRs present in the cells, whereas the electrophysiological experiments would record currents from the GlyRs present in the plasma membrane. Another explanation could be that the mutant GlyRs are incorrectly folded and/or nonfunctional, but still bind strychnine.

An unexpected corollary of the experiments related to the M287L mutation in the α1 GlyR subunit is that these mutants allow us to test the relevance of taurine to normal glycinergic transmission. We conclude that this role of taurine is probably minimal, given that α1(M287L) homomeric GlyRs are insensitive to taurine, and yet the glycinergic function in heterozygous $\alpha1^{M/L}$ knockin mice is not as compromised as in $\alpha1^{Q/I}$ knockin mice (Blednov et al., 2012).

The effect of ethanol on the α1(M287L) GlyRs expressed in oocytes showed variations in different batches of oocytes when carried out in normal buffer, at times exhibiting no differences from the WT, and at other times, a slight reduction. The experiments carried out in buffer to which 100 nM Zn^{2+} had been added showed that the Zn^{2+} enhancement of the ethanol potentiation is absent in the α1(M287L) GlyRs; therefore the variation observed in the normal buffer is probably caused by varying levels of existing Zn^{2+}. Reported levels of Zn^{2+} in buffers vary from low nanomolar to 1 μM, but in our buffer, Zn^{2+} levels were 30 nM or less (McCracken et al., 2010b). In our recordings from neurons (carried out in the presence of existing levels of Zn^{2+}), the ethanol effect was reduced in neurons from both heterozygous and homozygous M287L mice.

The absence of alcohol modulation in α1(Q266I) GlyR was remarkable, both in *X. laevis* oocytes and neurons. It is also noteworthy that, even though the Zn^{2+} potentiation of glycine responses was normal, adding Zn^{2+} to the buffer did not restore the ethanol or butanol effects.

Given the severe impairment of the glycinergic transmission observed in these mutants, it would be expected that another important inhibitory neurotransmitter, such as GABA, could provide some compensation. For instance, *spastic* mice (where the α1β GlyRs density is drastically reduced as a consequence of a mutation in the β subunit) show an increase in flunitrazepam binding (White and Heller, 1982) and an increase in the amplitude of $GABA_A$-mediated currents in dorsal horn (Graham et al., 2003), reflecting compensatory increases in the GABAergic transmission. However, the muscimol-mediated chloride uptake in synaptoneurosomes of spinal cord and brain stem from heterozygous α1(S267Q) knockin mice is the same as in WT mice (Findlay et al., 2003). *Oscillator* mice, where the number of α1β GlyR is also greatly reduced, do not show alterations in the amplitude of $GABA_A$-mediated currents in dorsal horn (Graham et al., 2003), indicating that in these cases, there is no compensatory change in the GABAergic transmission. In our study, we did not see any evidence of compensatory changes involving the $GABA_A$ receptor, because there were no changes in flunitrazepam binding in spinal cord and brain stem from homozygous $\alpha1^{Q/I}$ mice compared with WT.

Our previous experience with mutations in the GlyR that were shown to affect a putative binding cavity, but were lethal to the homozygous mice (Findlay et al., 2003), led us to ask whether mutations that were less directly involved in these critical sites might be more tolerated in vivo. However, this was not the case; the impairment of function observed in recombinant systems, which we initially considered moderate, was apparently sufficient to produce lethality in homozygous mice. The homology models of these mutations shed some light on this pattern of toxicity: we have postulated that interior cavities filled with water molecules are an important element for function of ligand-gated ion channels (Trudell and Harris, 2004), and ethanol could displace these molecules and affect gating. Here, we show that these mutations, especially Q266I, change the size and shape of the cavities within the TM domain. These changes in the size and shape of the cavity could possibly lead to the obliteration of alcohol modulation in the Q266I mutant GlyR.

It is noteworthy that previous research has shown that the length of the alcohol hydrophobic chain can lead to different changes in alcohol modulation when a particular amino acid is mutated. For instance, experiments in the prokaryotic GLIC channel showed that short- and long-chain alcohols interact differently with the amino acids lining the cavity, so different mutations will have differential effects on alcohol modulation according to the length of the hydrophobic chain (Howard et al., 2011). Of course, this may well be caused by the existence of more than one cavity where alcohol binds. In our particular case, both amino acids seem to be lining the same cavity, located within the TMs. But short- and long-chain alcohols will interact differently with the diverse amino acids lining the cavity, and that disparity will result in divergent changes in the modulation by alcohols of different chain length. The cavity volume is a determinant factor in the alcohol effect, but it is probably not the only one.

In summary, we studied two mutations in the GlyR α1 subunit, M287L and Q266I, and found that many of the basic characteristics, such as channel properties, present in mutated GlyRs expressed in *X. laevis* oocytes and HEK 293 cells were similar to those observed in isolated neurons and membrane preparations from the corresponding knockin mice: 1) a small but general impairment of glycine action, that is most evident in the glycine-induced maximal currents, and 2) lack of sensitivity to ethanol. The behavioral tests of the knockin mice (Blednov et al., 2012) reflect and expand some of these observations.

Acknowledgments

C.M.B. and R.A.H. thank Dr. Rebecca J. Howard and Kathryn Ondricek for construction of the Q266I mutant cDNA and Chelsea Geil, Brianne Patton, and Virginia Bleck for excellent technical assistance. S.V.I. and G.H. thank Carolyn Ferguson and Ed Mallick for expert technical assistance.

Authorship Contributions

Participated in research design: Mihic, Lovinger, Homanics, and Harris.

Conducted experiments: Borghese, Blednov, Quan, Iyer, Xiong, Trudell, and Homanics.

Performed data analysis: Borghese, Quan, Xiong, Mihic, Trudell, and Homanics.

Wrote or contributed to the writing of the manuscript: Borghese, Iyer, Mihic, Zhang, Lovinger, Trudell, Homanics, and Harris.

References

Alifimoff JK, Firestone LL, and Miller KW (1989) Anaesthetic potencies of primary alkanols: implications for the molecular dimensions of the anaesthetic site. *Br J Pharmacol* **96:**9–16.

Becker K, Breitinger HG, Humeny A, Meinck HM, Dietz B, Aksu F, and Becker CM (2008) The novel hyperekplexia allele GLRA1(S267N) affects the ethanol site of the glycine receptor. *Eur J Hum Genet* **16:**223–228.

Blednov YA, Benavidez JM, Homanics GE, and Harris RA (2012) Behavioral characterization of knockin mice with mutations M287L and Q266I in the glycine receptor α1 subunit. *J Pharmacol Exp Ther* **340:**317–329.

Bocquet N, Nury H, Baaden M, Le Poupon C, Changeux JP, Delarue M, and Corringer PJ (2009) X-ray structure of a pentameric ligand-gated ion channel in an apparently open conformation. *Nature* **457:**111–114.

Boehm SL 2nd, Peden L, Harris RA, and Blednov YA (2004) Deletion of the fyn-kinase gene alters sensitivity to GABAergic drugs: dependence on β2/β3 GABAA receptor subunits. *J Pharmacol Exp Ther* **309:**1154–1159.

Breitinger HG, Lanig H, Vohwinkel C, Grewer C, Breitinger U, Clark T, and Becker CM (2004) Molecular dynamics simulation links conformation of a pore-flanking region to hyperekplexia-related dysfunction of the inhibitory glycine receptor. *Chem Biol* **11:**1339–1350.

Buckwalter MS, Cook SA, Davisson MT, White WF, and Camper SA (1994) A frameshift mutation in the mouse α1 glycine receptor gene (Glra1) results in progressive neurological symptoms and juvenile death. *Hum Mol Genet* **3:**2025–2030.

Castaldo P, Stefanoni P, Miceli F, Coppola G, Del Giudice EM, Bellini G, Pascotto A, Trudell JR, Harrison NL, Annunziato L, et al. (2004) A novel hyperekplexia-causing mutation in the pre-transmembrane segment 1 of the human glycine receptor α1 subunit reduces membrane expression and impairs gating by agonists. *J Biol Chem* **279:**25598–25604.

Celentano JJ, Gibbs TT, and Farb DH (1988) Ethanol potentiates GABA- and glycine-induced chloride currents in chick spinal cord neurons. *Brain Res* **455:**377–380.

Chung SK, Vanbellinghen JF, Mullins JG, Robinson A, Hantke J, Hammond CL, Gilbert DF, Freilinger M, Ryan M, Kruer MC, et al. (2010) Pathophysiological mechanisms of dominant and recessive GLRA1 mutations in hyperekplexia. *J Neurosci* **30:**9612–9620.

Duret G, Van Renterghem C, Weng Y, Prevost M, Moraga-Cid G, Huon C, Sonner JM, and Corringer PJ (2011) Functional prokaryotic-eukaryotic chimera from the pentameric ligand-gated ion channel family. *Proc Natl Acad Sci U S A* **108:**12143–12148.

Ernst M, Bruckner S, Boresch S, and Sieghart W (2005) Comparative models of GABAA receptor extracellular and transmembrane domains: important insights in pharmacology and function. *Mol Pharmacol* **68:**1291–1300.

Findlay GS, Phelan R, Roberts MT, Homanics GE, Bergeson SE, Lopreato GF, Mihic SJ, Blednov YA, and Harris RA (2003) Glycine receptor knock-in mice and hyperekplexia-like phenotypes: comparisons with the null mutant. *J Neurosci* **23:**8051–8059.

Findlay GS, Wick MJ, Mascia MP, Wallace D, Miller GW, Harris RA, and Blednov YA (2002) Transgenic expression of a mutant glycine receptor decreases alcohol sensitivity of mice. *J Pharmacol Exp Ther* **300:**526–534.

Graham BA, Schofield PR, Sah P, and Callister RJ (2003) Altered inhibitory synaptic transmission in superficial dorsal horn neurones in spastic and oscillator mice. *J Physiol* **551:**905–916.

Harvey RJ, Topf M, Harvey K, and Rees MI (2008) The genetics of hyperekplexia: more than startle! *Trends Genet* **24:**439–447.

Hirzel K, Müller U, Latal AT, Hülsmann S, Grudzinska J, Seeliger MW, Betz H, and Laube B (2006) Hyperekplexia phenotype of glycine receptor α1 subunit mutant mice identifies Zn^{2+} as an essential endogenous modulator of glycinergic neurotransmission. *Neuron* **52:**679–690.

Homanics GE, Ferguson C, Quinlan JJ, Daggett J, Snyder K, Lagenaur C, Mi ZP, Wang XH, Grayson DR, and Firestone LL (1997) Gene knockout of the α6 subunit of the γ-aminobutyric acid type A receptor: lack of effect on responses to ethanol, pentobarbital, and general anesthetics. *Mol Pharmacol* **51:**588–596.

Howard RJ, Murail S, Ondricek KE, Corringer PJ, Lindahl E, Trudell JR, and Harris RA (2011) Structural basis for alcohol modulation of a pentameric ligand-gated ion channel. *Proc Natl Acad Sci U S A* **108:**12149–12154.

Kling C, Koch M, Saul B, and Becker CM (1997) The frameshift mutation oscillator (Glra1(spd-ot)) produces a complete loss of glycine receptor α1-polypeptide in mouse central nervous system. *Neuroscience* **78:**411–417.

Langosch D, Laube B, Rundström N, Schmieden V, Bormann J, and Betz H (1994) Decreased agonist affinity and chloride conductance of mutant glycine receptors associated with human hereditary hyperekplexia. *EMBO J* **13:**4223–4228.

Liu J, Wu DC, and Wang YT (2010) Allosteric potentiation of glycine receptor chloride currents by glutamate. *Nat Neurosci* **13:**1225–1232.

Lobo IA, Harris RA, and Trudell JR (2008) Cross-linking of sites involved with alcohol action between transmembrane segments 1 and 3 of the glycine receptor following activation. *J Neurochem* **104:**1649–1662.

Lynch JW (2009) Native glycine receptor subtypes and their physiological roles. *Neuropharmacology* **56:**303–309.

Mascia MP, Mihic SJ, Valenzuela CF, Schofield PR, and Harris RA (1996) A single amino acid determines differences in ethanol actions on strychnine-sensitive glycine receptors. *Mol Pharmacol* **50:**402–406.

Mascia MP, Trudell JR, and Harris RA (2000) Specific binding sites for alcohols and anesthetics on ligand-gated ion channels. *Proc Natl Acad Sci U S A* **97:**9305–9310.

McCracken LM, McCracken ML, Gong DH, Trudell JR, and Harris RA (2010a) Linking of glycine receptor transmembrane segments three and four allows assignment of intrasubunit-facing residues. *ACS Chem Neurosci* **1:**482.

McCracken LM, Trudell JR, Goldstein BE, Harris RA, and Mihic SJ (2010b) Zinc enhances ethanol modulation of the α1 glycine receptor. *Neuropharmacology* **58:**676–681.

Meyers EN, Lewandoski M, and Martin GR (1998) An Fgf8 mutant allelic series generated by Cre- and Flp-mediated recombination. *Nat Genet* **18:**136–141.

Mihic SJ, Ye Q, Wick MJ, Koltchine VV, Krasowski MD, Finn SE, Mascia MP, Valenzuela CF, Hanson KK, Greenblatt EP, et al. (1997) Sites of alcohol and volatile anaesthetic action on GABA(A) and glycine receptors. *Nature* **389:**385–389.

Moorhouse AJ, Jacques P, Barry PH, and Schofield PR (1999) The startle disease mutation Q266H, in the second transmembrane domain of the human glycine receptor, impairs channel gating. *Mol Pharmacol* **55:**386–395.

Nagy A, Rossant J, Nagy R, Abramow-Newerly W, and Roder JC (1993) Derivation of completely cell culture-derived mice from early-passage embryonic stem cells. *Proc Natl Acad Sci U S A* **90:**8424–8428.

Plested AJ, Groot-Kormelink PJ, Colquhoun D, and Sivilotti LG (2007) Single-channel study of the spasmodic mutation α1A52S in recombinant rat glycine receptors. *J Physiol* **581:**51–73.

Ponder JM and Richards FM (1987) Tertiary templates for proteins. Use of packing criteria in the enumeration of allowed sequences for different structural classes. *J Mol Biol* **193:**775–791.

Rajendra S, Lynch JW, Pierce KD, French CR, Barry PH, and Schofield PR (1995) Mutation of an arginine residue in the human glycine receptor transforms β-alanine and taurine from agonists into competitive antagonists. *Neuron* **14:**169–175.

Rodríguez CI, Buchholz F, Galloway J, Sequerra R, Kasper J, Ayala R, Stewart AF, and Dymecki SM (2000) High-efficiency deleter mice show that FLPe is an alternative to Cre-loxP. *Nat Genet* **25:**139–140.

Saul B, Schmieden V, Kling C, Mülhardt C, Gass P, Kuhse J, and Becker CM (1994) Point mutation of glycine receptor α1 subunit in the spasmodic mouse affects agonist responses. *FEBS Lett* **350:**71–76.

Trudell JR and Harris RA (2004) Are sobriety and consciousness determined by water in protein cavities? *Alcohol Clin Exp Res* **28:**1–3.

Villmann C, Oertel J, Melzer N, and Becker CM (2009) Recessive hyperekplexia mutations of the glycine receptor α1 subunit affect cell surface integration and stability. *J Neurochem* **111:**837–847.

Welsh BT, Goldstein BE, and Mihic SJ (2009) Single-channel analysis of ethanol enhancement of glycine receptor function. *J Pharmacol Exp Ther* **330:**198–205.

Werner DF, Swihart A, Rau V, Jia F, Borghese CM, McCracken ML, Iyer S, Fanselow MS, Oh I, Sonner JM, et al. (2011) Inhaled anesthetic responses of recombinant receptors and knockin mice harboring α2(S270H/L277A) GABA(A) receptor subunits that are resistant to isoflurane. *J Pharmacol Exp Ther* **336:**134–144.

White WF and Heller AH (1982) Glycine receptor alteration in the mutant mouse spastic. *Nature* **298:**655–657.

Address correspondence to: R. Adron Harris, Waggoner Center for Alcohol and Addiction Research, The University of Texas at Austin, 1 University Station, A4800, Austin, TX 78712-0159. E-mail: harris@mail.utexas.edu.